



# The effect of gas migration on the deformation and permeability of coal under the condition of true triaxial stress

Gang Wang<sup>1,2,3</sup> · Zhiyuan Liu<sup>2</sup> · Pengfei Wang<sup>2</sup> · Yangyang Guo<sup>2</sup> · Wenrui Wang<sup>2</sup> · Tengyao Huang<sup>2</sup> · Wenxin Li<sup>2</sup>

Received: 10 October 2018 / Accepted: 10 July 2019 / Published online: 1 August 2019  
© Saudi Society for Geosciences 2019

## Abstract

The dynamic characteristics of gas flow are often not considered in a true triaxial stress environment, making the simulation test hard to meet the requirement for coal and gas outburst in reality. To solve this issue, we investigated the deformation and gas flow characteristics of coal-like briquette under true triaxial stress conditions using self-developed triaxial servo-controlled seepage equipment for fluid-solid coupling of coal containing methane. Analysis of the experimental data revealed the relationship of coal body's stress to strain as well as the relationship of their permeability. The results showed that in the conventional triaxial and true triaxial compression seepage tests, the relationship of stress-strain-permeability varies at different stages. The stress-strain curves in the whole stress-strain process of coal show a trend of decrease after increase, while the permeability-strain curves show a trend of increase after decrease. There is a "stress-sensitive zone" in the influence of the intermediate principal stress on the minimum permeability of the coal. The gas pressure promotes the "fluctuation" strain of the coal body, resulting in an instantaneous increase in the strain rate. The research provides the experimental basis for studying the permeability of coal body in the true triaxial stress environment.

**Keywords** Coal mine methane drainage · True triaxial test · Intermediate principal stress · Gas pressure · Permeability

## Introduction

Coal and gas outburst is an extremely complex gas dynamic phenomenon encountered in the production of underground coal mine and characterized as sudden eruption of a large amount of gas and coal from the coal tunnel or stope within a very short period of time (Hu et al. 2013). Therefore, to effectively reduce the adverse effects of ground stress and

gas on coal mining, their influence on mechanical properties and permeability of coal rock mass has become a hot research topic.

Many scholars have studied the compressive strength and deformation and permeability of coal and rock under conventional triaxial stress (maximum principal stress  $\sigma_1 >$  intermediate principal stress  $\sigma_2 =$  minimum principal stress  $\sigma_3$ ) and explored the deformation and seepage characteristics of coal under different axial pressure, confining pressure, and pore pressure (Chen et al. 2012; Jasinge et al. 2011; Mavor and Gunter 2006). With the improvement of test equipment and test methods, scholars begin to study the influence of various factors such as temperature, water content, and pore fissure structure on the permeability of coal body under the complicated loading and unloading stress path, such as variable axial pressure and variable confining pressure (Jasinge et al. 2011; Liu et al. 2010, 2018; Xu et al. 2010; Yin et al. 2010, 2012, 2015, 2017). However, field stress distribution of coal seam is very complex. Under certain extreme conditions, the triaxial stress may vary greatly. The conventional triaxial tests often neglect the effects of intermediate principal stress and cannot reflect the field complex ground stress conditions. Therefore, true triaxial tests ( $\sigma_1 > \sigma_2 > \sigma_3$ ) should be conducted at the

---

Editorial handling: Liang Xiao

✉ Gang Wang  
gang.wang@sdust.edu.cn

<sup>1</sup> Mine Disaster Prevention and Control-Ministry of State Key Laboratory Breeding Base, Shandong University of Science and Technology, 579 Qianwangang Rd, Huangdao District, Qingdao 266510, China

<sup>2</sup> College of Mining and Safety Engineering, Shandong University of Science and Technology, Room 108, 579 Qianwangang Rd, Huangdao District, Qingdao 266510, China

<sup>3</sup> Hebei State Key Laboratory of Mine Disaster Prevention, North China Institute of Science and Technology, Beijing 101601, China

laboratory conditions. Some of the scholars have taken the rock as the research object and used the true triaxial test device to study the influence of the intermediate principal stress, temperature, and osmotic pressure on the permeability, compressive strength, and deformation of rock mass (Haimson and Chang 2000; Li et al. 2016a, b; Lombos et al. 2013; Wang et al. 2017a, b) and the effects of the intermediate principal stress on the mechanical properties of coal mass (Mogi 1967, 1971; Pan et al. 2012). Pan and Meng et al. experimentally explored the influence of the intermediate principal stress and the osmotic pressure on the permeability of coal by using the real triaxial test system (Meng et al. 2015; Pan et al. 2012).

So far, the true triaxial tests are mainly limited to the study of mechanical properties of rock. Very few studies have explored gas seepage of coal body under true triaxial stress. Gas pressure is the internal pore pressure of coal and often varies in different areas of coal seam (Chen et al. 2019). Its influence on the mechanical and seepage characteristics of coal body has been extensively studied (Wang et al. 2019). Li and Qin et al. carried out the creep characteristics and the acoustic emission characteristics of coal under triaxial compression under different gas pressures (Li et al. 2018; Qin et al. 2013). Cao et al. used the triaxial osmosis apparatus developed by the laboratory to test the seepage characteristics of the coal outburst under different axial pressures confining pressure (Cao et al. 2010). Wang et al. analyzed the variation of coal permeability characteristics during the change of gas pressure using gas permeation meter (Cheng et al. 2018; Wang et al. 2012; Zhang et al. 2015). Wang et al. tested the gas permeability under different pressures and temperature using a self-developed coal rock steady-state permeability test system (Wang et al. 2017a, b).

Although many scholars have intensively studied the law of coal permeability changes and the rock mechanics characteristics under conventional triaxial stress, these tests did not consider the impacts of dynamic gas seepage on coal and gas outburst under the condition of true triaxial stress. Since gas seepage is an important factor affecting coal and gas outbursts, in this study, we explored the seepage characteristics of different gas pressure briquettes under the condition of true triaxial stress with the help of the self-developed true triaxial gas-solid coupled coal seepage test system, which is of positive significance for understanding the effect of permeability of coal on the coal and gas outburst.

## Materials, instruments, and methods

### Materials and sample preparation

Coal samples were taken from no. 8 coal seam at Yuyang Coal Mine of Chongqing Songzao Coal and Electricity Co., Ltd.

Their industry indexes have been reported previously (Wang et al. 2017a, b). Because processing raw coal samples in the soft and brittle coal seam is very difficult and the anisotropic heterogeneous characteristics of large random samples often result in different mechanical properties and permeability (Dutka 2019; He et al. 2018; Ding and Yue 2018), which do not meet the basic requirements of the test for coal samples, the homogeneous coal briquette specimens are used for the tests (Yin et al. 2016). In brief, pulverized original coal samples were sieved to obtain a total of 2.55 kg equivalent coal powder of 20–40 mesh and 40–80 mesh. After uniformly mixed with water, the coal powder mud was shaped in the especially designed specimen molds for 30 min under the pressure of 100 MPa provided using a 100-t press and prepared as rectangular cubic samples of 100 mm × 100 mm × 200 mm in size. The processed samples were placed in an 80 °C oven for 24 h and wrapped with plastic film for testing (Wang et al. 2018). The production process of coal samples is shown in Fig. 1.

### Experiment setup

The experiments were conducted using a true triaxial gas-solid coupling coal seepage testing device developed independently by Shandong University of Science and Technology (Wang et al. 2018). The test system was mainly composed of a true triaxial pressure chamber, a hydraulic servo system, a gas seepage system, and a monitoring and control system. Figure 2 shows the schematic of its operation principle. The device could provide the maximum axial principal stress ( $\sigma_1$ ) of 70 MPa, the maximum lateral intermediate principal stress ( $\sigma_2$ ) of 35 MPa, minimum principal stress ( $\sigma_3$ ) of 10 MPa, the maximum gas pressure of 6 MPa, the maximum axial displacement of 50 mm, and the maximum lateral displacement (unilateral) of 30 mm (Li et al. 2016a, b). Among the three principal stresses,  $\sigma_1$  and  $\sigma_2$  were loaded using rigid pressure heads and  $\sigma_3$  was supplied using the hydraulic oil loading, realizing an independent loading  $\sigma_1$  and  $\sigma_2$  and  $\sigma_3$  in three directions without disturbing one another, and carry on the tests of coal body gas permeation under different loading and unloading paths as well as conventional triaxial and true triaxial stress conditions.

### Testing methods and procedures

In order to realize the experimental study of coal gas seepage under different intermediate principal stress conditions, different intermediate principal stress environments were set up. During the experiment, first, the major, intermediate, and minor principal stresses  $\sigma_1$ ,  $\sigma_2$ , and  $\sigma_3$  were loaded to the pre-set values and kept them invariant. Then, the gas of 99% in concentration was filled. When

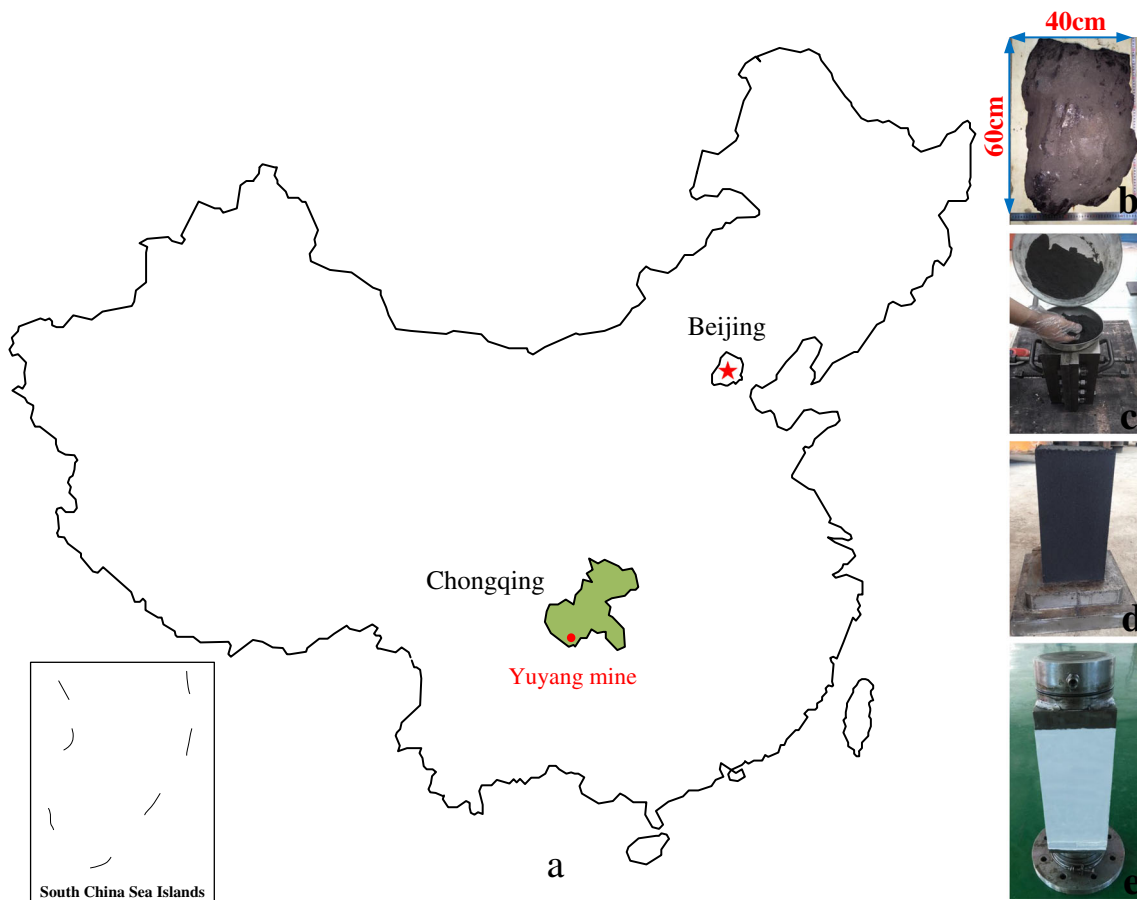


**Fig. 1** Coal sample making process. (a) the location of Yuyang Mine, (b) raw coal, (c) filling of molds, (d) forming coal samples, (e) test coal samples

the gas flow in the coal body is stable, which was reached when the indicator of gas flow accumulator does not change or the time flow curve tends to be horizontal, the axial stress was continuously applied to the specimen until it failed to observe the experiment process and was simultaneously monitored for gas flow and coal sample deformation displacement, the effects of the coupling action of true triaxial stress, and gas pressure on the mechanical characteristics of the coal sample under and the characteristics of gas seepage in the sample. Table 1 lists the related experimental loading parameters.

Assuming that the seepage process of gas in coal during the experiment is an isothermal process, the molded coal is an isotropic homogeneous material, and the gas seepage in the coal obeys the Darcy’s law, the average permeability  $K$  of the gas-bearing coal can be expressed as:

$$K = \frac{2q\mu LP_n}{A(P_1^2 - P_2^2)}$$

where  $K$  is the permeability ( $m^2$ ),  $q$  is the gas seepage velocity of coal mass ( $m^3/s$ ),  $\mu$  is the dynamic viscosity

coefficient of gas (it is usually taken as  $1.087 \times 10^{-11}$  MPa s),  $L$  is the length of the coal sample (m),  $P_n$  is the atmospheric pressure (MPa),  $A$  is the cross-sectional area of the sample ( $m^2$ ),  $P_1$  is the pressure of gas at the inlet (MPa), and  $P_2$  is the pressure of gas at the outlet (MPa).

### Results and discussion

Figure 3 is the stress-strain curves and permeability-stress curves of the coal body during the full stress-strain process under conventional triaxial and true triaxial stress conditions. In the conventional triaxial compression process,  $\sigma_3$  is equal to  $\sigma_2$ , which is constant at 4 MPa, and  $\sigma_1$  is continuously loaded until the end of the test. At the same time,  $\sigma_3$  is maintained at 4 MPa,  $\sigma_2$  is 6 MPa, and  $\sigma_1$  is continuously loaded until the end of the test in the true triaxial compression process.

Figure 3 shows the stress-strain-permeability curves of coal subject to different initial stresses (where  $\Delta\sigma$  is  $\sigma_1 - \sigma_3$ ; the compression deformation of coal is positive and the expansion deformation is negative). From the figure, it is clear that under a constant gas pressure (1 MPa),

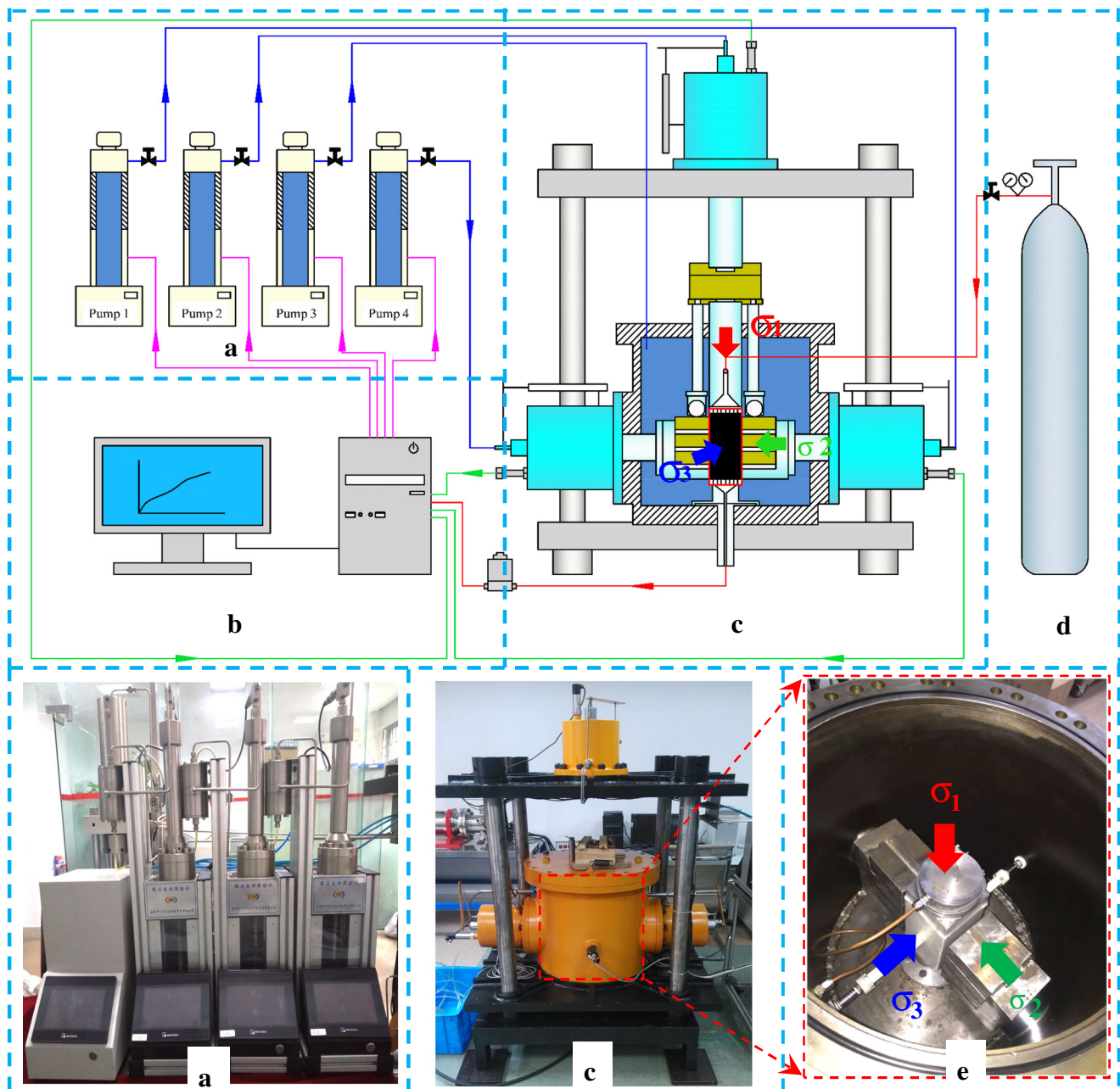


**Fig. 2** Testing system schematic. (a) Hydraulic servo system, (b) monitoring and control system, (c) true triaxial pressure chamber, (d) gas cylinders, and (e) internal structure of triaxial pressure chamber

the coal's stress-strain process can be divided roughly into four stages: the initial compaction stage (stage I:  $\Delta\sigma$  increases from 0 to  $\sim 3$  MPa), elastic deformation stage (stage II:  $\Delta\sigma$  increases from 3 to  $\sim 15$  MPa), plastic deformation stage (stage III:  $\Delta\sigma$  increases from  $\sim 15$  MPa to  $\sim 24$  MPa), and destruction instability stage (stage IV: after  $\sim 24$  MPa). In stage I, with the increase of axial pressure, the primary microscopic pores and fractures inside the coal specimen are gradually compacted to closure, leading to a decrease in porosity and gas seepage passageways. Therefore, the gas flow is blocked and gas

permeability displays a gradual decrease trend, forming the early nonlinear deformation phenomenon. With the increase of  $\sigma_2$ , the compaction becomes less and less obvious. In stage II, the specimen mainly undergoes elastic deformation. The stress-strain curve is approximately a linear one. The primary microscopic pores and fractures are further compacted due to action of the axial stress, resulting in a further reduction in porosity and a continuous lowering in permeability. With the increase of axial strain, the rate of decrease in permeability gradually decreases. In stage III, the internal damage of the coal



**Table 1** Initial load parameters

Serial number	Initial $\sigma_1$ /MPa	Initial $\sigma_2$ /MPa	Initial $\sigma_3$ /MPa	Gas pressure P/MPa
1	4	4	4	0.5
2	4	4	4	1.0
3	4	4	4	1.5
4	6	6	4	0.5
5	6	6	4	1.0
6	6	6	4	1.5
7	8	8	4	0.5
8	8	8	4	1.0
9	8	8	4	1.5

sample leads to a corresponding decrease in the bearing capacity. At this time, new cracks are continuously generated inside the coal sample, the damage continues to develop, and the stress-strain curve begins to deviate from the straight line. Although the axial stress continues to increase, its increase rate gradually decreases. But because these fractures do not cut through, the gas seepage passageways continue to narrow down, further decreasing gas permeability to its minimum when reaching the compressive strength. In stage IV, the specimen is subjected to rapid stress falling, which is the macroscopic manifestation of the transition from the primary continuous damage and uniform strain to the localized damage and internal strain accumulation. Its essence is the instable expansion of internal pores and fractures. In this stage, microfractures cluster, conglomerate, and penetrate inside the specimen, leading to consecutive enlargement of gas seepage passageways and increased permeability. However, due to the squeezing, pressing, and dislocating of coal particles, the newly generated fractures are blocked or clogged, resulting in only slight increase in permeability. The above analysis clearly indicates that the change in permeability of coal specimen is closely related to its deformation and damage characteristics.

As shown in Fig. 3, the three-direction strain changes with the increase of the principal stress difference in the two stress states. In the conventional triaxial compression test,  $\sigma_3$  and the change trend of  $\sigma_2$  direction are the same, that is, the coal body in these two directions first undergoes compression deformation after the expansion deformation, and at  $\sigma_1$  direction always undergoes compression deformation. By contrast, in the true triaxial compression test, the coal body at the direction of  $\sigma_2$  always undergoes compression deformation. From the analysis of the whole stress-strain process of coal body, the ability of coal body to resist deformation is enhanced and the permeability is decreased under true triaxial stress environment.

## Effect of intermediate principal stress on mechanical and permeability characteristics of coal samples

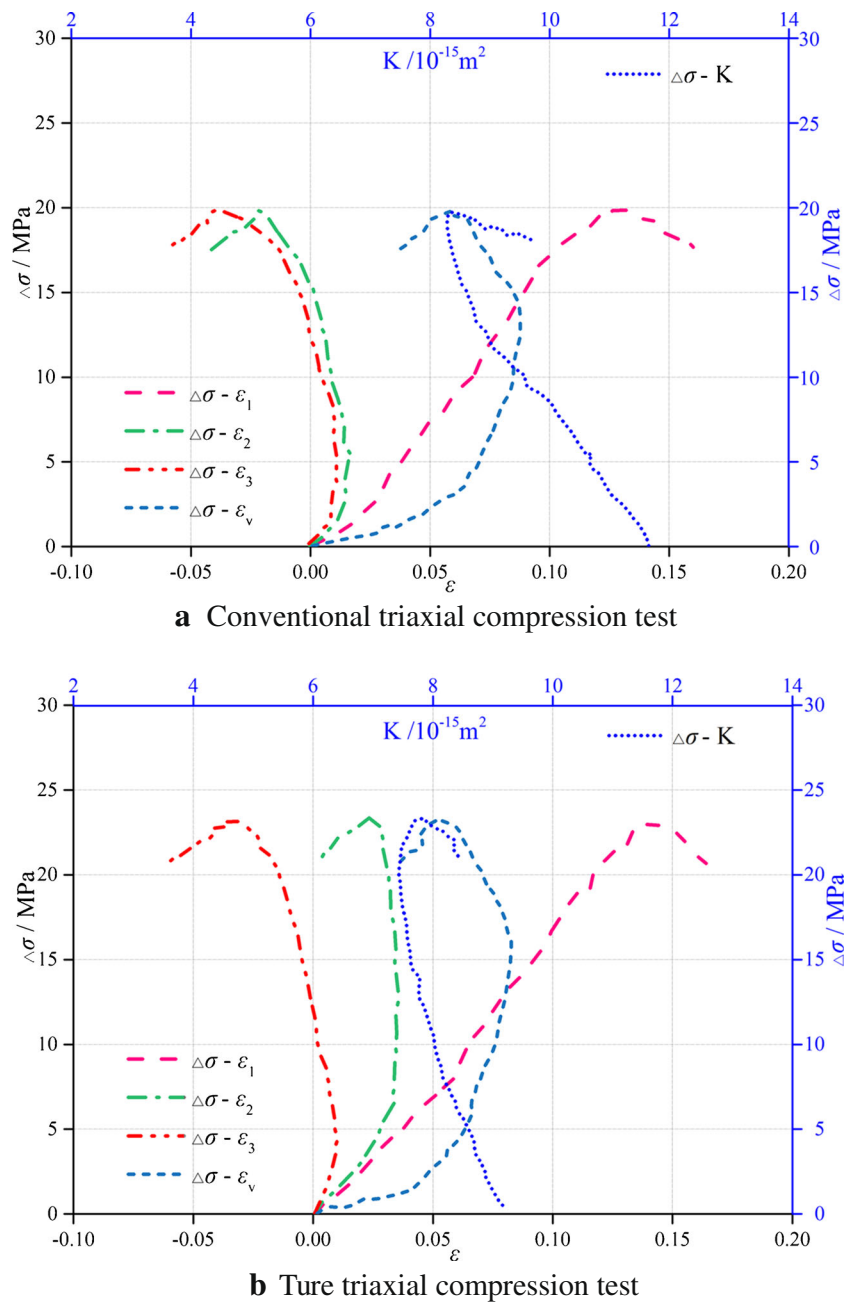
The stress-strain curves and permeability curves of coal samples under different intermediate principal stresses are shown in Fig. 4. It can be seen from the diagram that the stress and strain of the coal sample show a tendency of decrease after increase with strain increasing, while the gas permeability shows a tendency of increases after decrease with the strain increasing.

From Fig. 5, when  $P$  (gas pressure) is 0.5 MPa, with  $\sigma_2$  increasing from 4 MPa to 6 MPa and 8 MPa,  $\sigma_u$  (the compressive strength of coal) increased by 19.6% and 27.5%, respectively. When reaching  $\sigma_u$ , the produced strain  $\varepsilon_u$  at  $\sigma_1$  direction decreased by 14.3% and 28.6%, respectively. And  $K_{\max}$  (the maximum permeability) decreased by 21.4% and 44.4%, respectively, and  $K_{\min}$  (the minimum permeability) decreased by 37.1% and 71.5%. Similarly, the stress strain and permeability of three kinds of  $\sigma_2$  showed similar changes when  $P = 1.0$  MPa and 1.5 MPa. It is shown that under the same gas pressure, the change trend of the two curves is the same and the main effects of intermediate principal stress on coal samples are as follows: (1) the intermediate principal stress changes the compressive strength of the coal body (Wenshuai et al. 2019; Wang and Qian 2018); (2) the intermediate principal stress changes the axial strain of coal sample; and (3) the middle principal stress restricts the development of coal fissure and reduces the effective channel of seepage.

The results show that the greater the  $\sigma_2$ , the greater the  $\sigma_u$  of coal, the smaller the corresponding axial strain when the compressive strength is reached, the smaller the  $K_{\max}$ . The reasons are as follows:

1. The  $\sigma_2$  has obstructed the expansion of the pores and fractures in the coal body. The greater the  $\sigma_2$ , the more easily the pore and fracture are compacted, the greater the ability of coal body to resist the elastic deformation, and the smaller the gas seepage channel. The binding effect of  $\sigma_2$  at 6 MPa and 8 MPa is higher than that in the direction of  $\sigma_2$  at 4 MPa, which makes the left and right tensile quantity different.
2. There are a lot of micro- and meso-pores in the coal sample, and the influence of the intermediate principal stress on the coal permeability is closely related to the internal structure of the specimen (Shi et al. 2018). At the same time, as a typical porous medium, the micro-fracture provides a channel for gas seepage, so the restriction of the intermediate principal stress and the fractures generated due to loading the maximum principal stress are the key factors affecting coal seepage characteristics.
3. In the process of  $\sigma_1$  loading, the  $K$  decreased obviously. Because of the joint action of  $\sigma_1$ ,  $\sigma_2$ , and  $\sigma_3$ , the microfractures are closed gradually in coal sample. Thus, the

**Fig. 3** Coal’s permeability and deformation  $\varepsilon_1, \varepsilon_2, \varepsilon_3$ , as well as the principal stress difference  $\Delta\sigma$  relation in conventional and true triaxial tests. (a) Conventional triaxial compression test and (b) True triaxial compression test

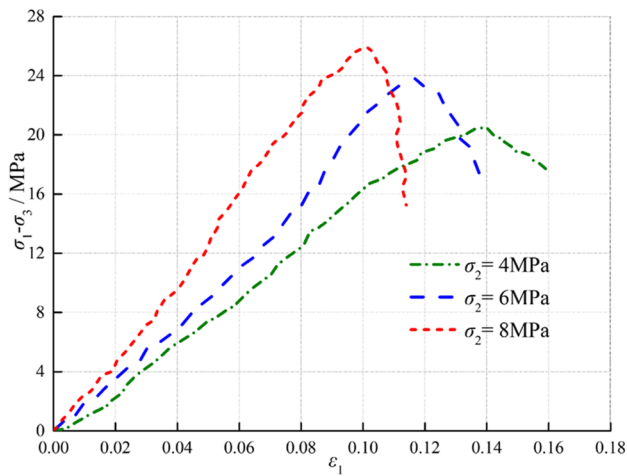


coal sample is compacted and its porosity is reduced. Therefore, the gas seepage channel narrows, the gas flow in the coal is hindered, and the permeability decreases. After the coal sample reaches the compressive strength, the macroscopic manifestation of starting continues damage and the uniform strain is transformed to localization of damage and strain, leading to instability expansion of the fractures. The internal micro-fractures gather together, assemble and penetrate in the specimen, leading to increased gas seepage channels and permeability. Since the pulverized coal particles have been separated from the specimen, the new cracks will be blocked. Thus, the permeability only shows a small increase.

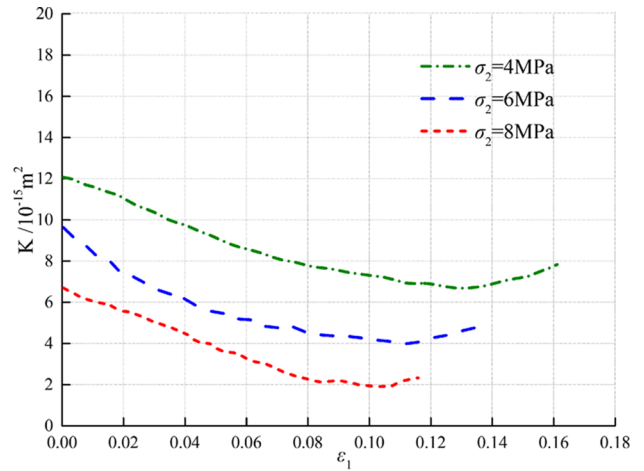
**Gas permeability characteristics of coal samples under different gas pressures**

The curves of stress and permeability of coal samples with strain changing under different gas pressure conditions are shown in Fig. 6. It can be seen from the figure that at the same intermediate principal stress, the changes of stress of coal sample with strain increasing under different gas pressure show a trend of decrease after increase, while the changes of permeability with strain increasing show a trend of increase after decrease.

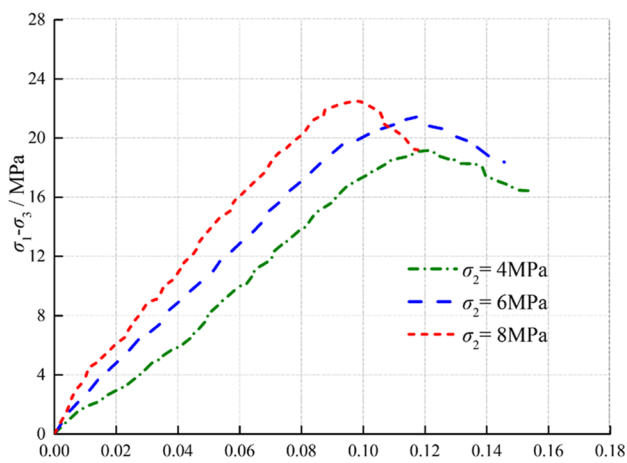
Further analysis of Fig. 7 shows that in the case of  $\sigma_2$  equaling to 4 MPa,  $P$  increased from 0.5 to 1.0 MPa and



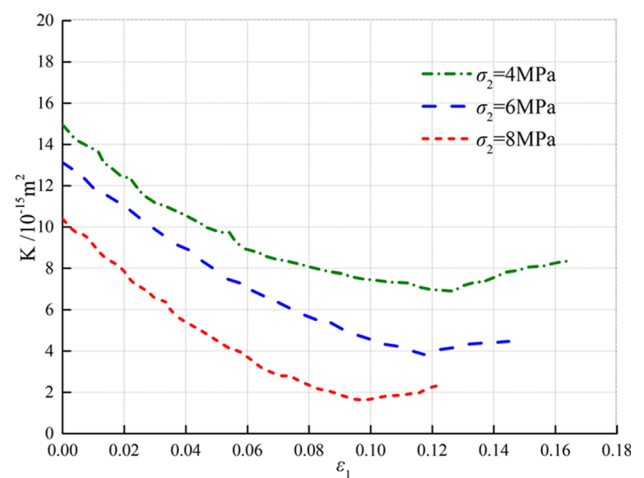
**a** Strain-stress curve of P-0.5 MPa



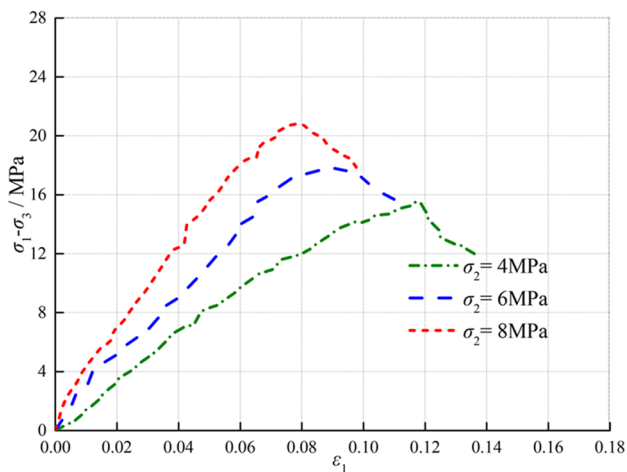
**b** Strain-permeability curve of P-0.5 MPa



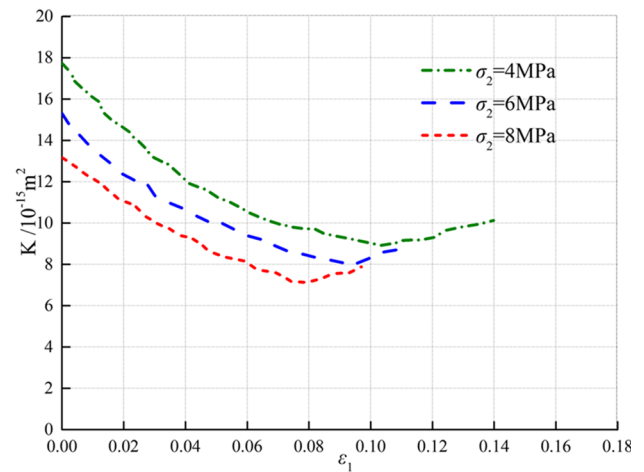
**c** Strain-stress curve of P-1.0 MPa



**d** Strain-permeability curve of P-1.0 MPa



**e** Strain-stress curve of P-1.5 MPa



**f** Strain-permeability curve of P-1.5 MPa

**Fig. 4** Axial stress-strain and strain-permeability curves of coal under different intermediate principal stresses. **a** Strain-stress curve of P-0.5 MPa. **b** Strain-permeability curve of P-0.5 MPa. **c** Strain-stress curve of

P-1.0 MPa. **d** Strain-permeability curve of P-1.0 MPa. **e** Strain-stress curve of P-1.5 MPa. **f** Strain-permeability curve of P-1.5 MPa

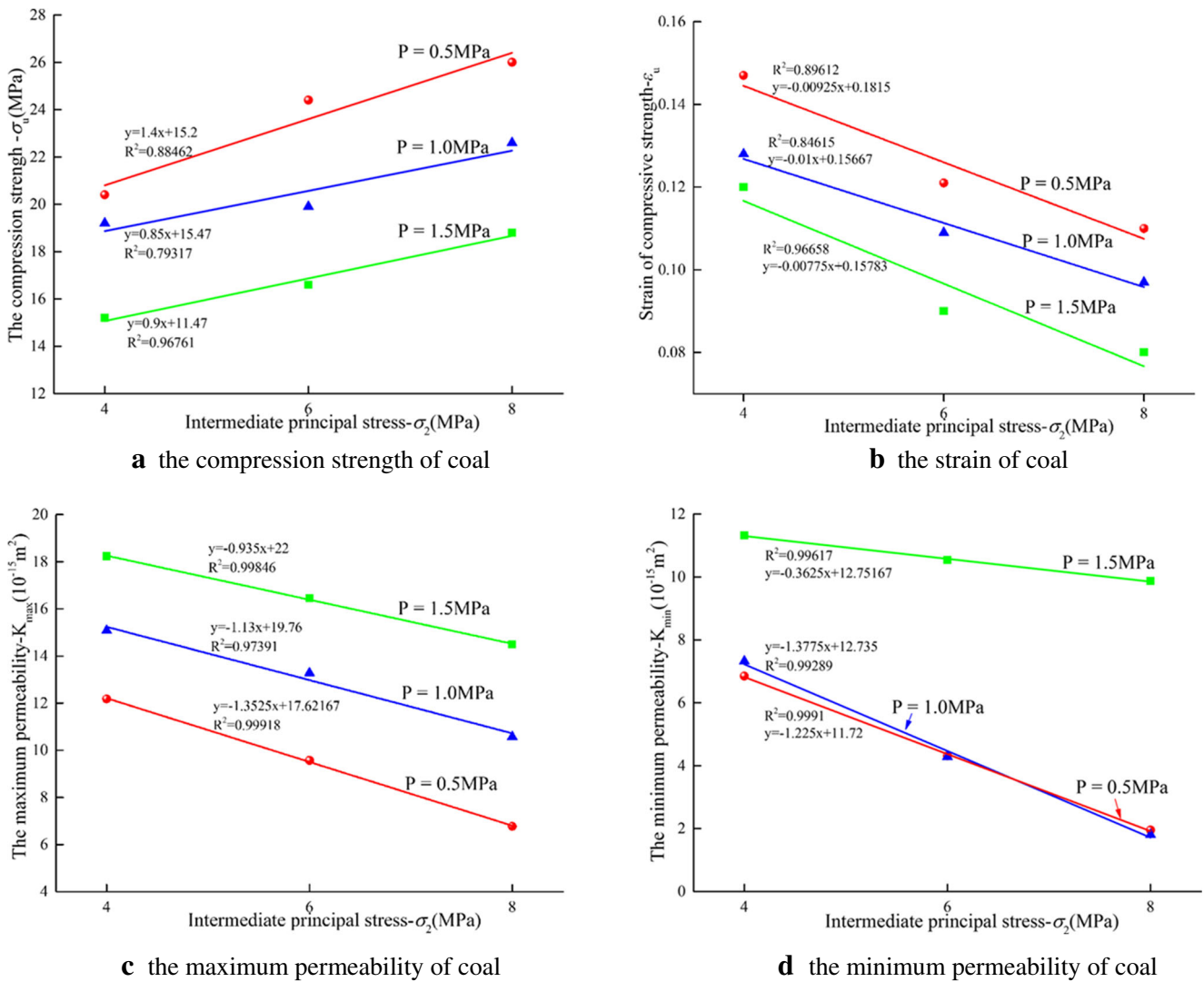


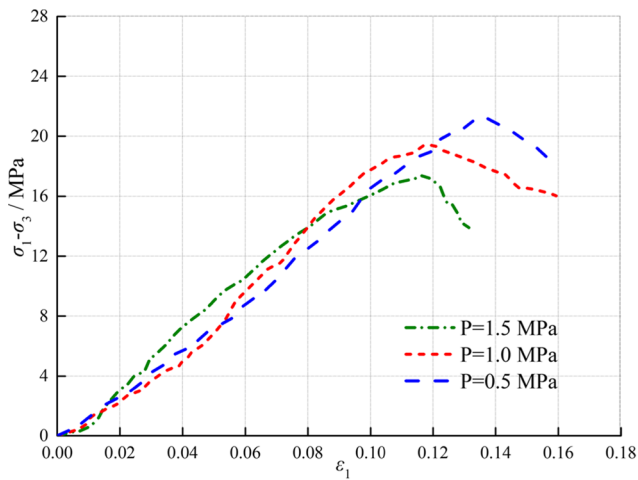
**Fig. 5** Influence of intermediate principal stress on coal mechanics and permeability characteristics. **a** The compression strength of coal. **b** The strain of coal. **c** The maximum permeability of coal. **d** The minimum permeability of coal

1.5 MPa,  $\sigma_u$  relative to that at  $P$  equaling to 4 MPa decreased by 5.8% and 25.5%, and the strain  $\epsilon_u$  reduced by 14.3% and 21.4%. In addition,  $K_{max}$  at  $P$  equaling to 1.0 MPa and 1.5 MPa relative to that at  $P$  equaling to 0.5 MPa increased by 23.8% and 33%, respectively. Similarly, the variation of stress and strain and permeability under three gas pressures under the condition of  $\sigma_2$  6 MPa and 8 MPa also shows that the change trend of the two curves is the same under the same intermediate principal stress. The main effects of gas pressure on coal samples are as follows: (1) the gas pressure reduces the compressive strength of the coal body; (2) the gas pressure changes the axial strain of coal sample; and (3) the gas pressure can promote the development of coal fissure and enlarge the effective channel of seepage.

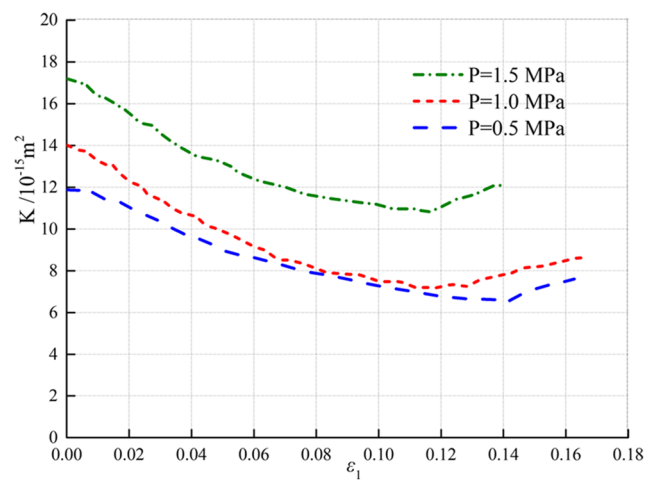
The mechanisms of action of gas pressure on coal permeability are as follows:

1. The gas in the pores and fractures of the coal body exists in two states: free and adsorbed. The former is present in a free form in the space among pores of the coal body, while the latter is adsorbed on the surface in a molecular state. The free gas generates a flow in the connected pores and fissures. At this time, the mechanical action of the gas fluid on the coal sample is applied to the coal body by the pore pressure in an effective stress manner; that is, the deformation and failure process of the coal body is effective and controlled by the effective stress. Under the action of stress, the pores and fissures of the coal body develop continuously. Under the specific true triaxial stress conditions, when the gas pressure is larger, the effective stress of the coal sample is smaller; fewer pores and cracks inside the coal body are closed and the gas flow rate through the coal body is greater during the time.

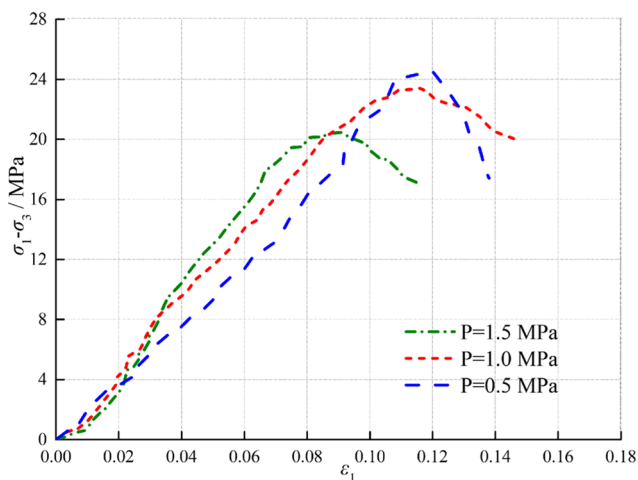




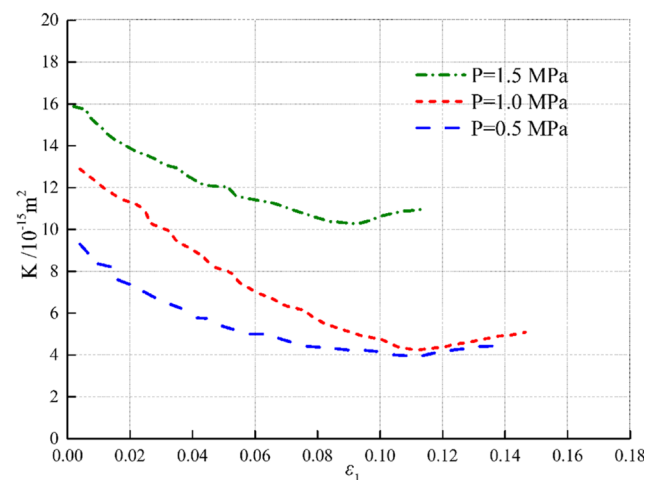
**a** Strain-stress curve of  $\sigma_2$ -4 MPa



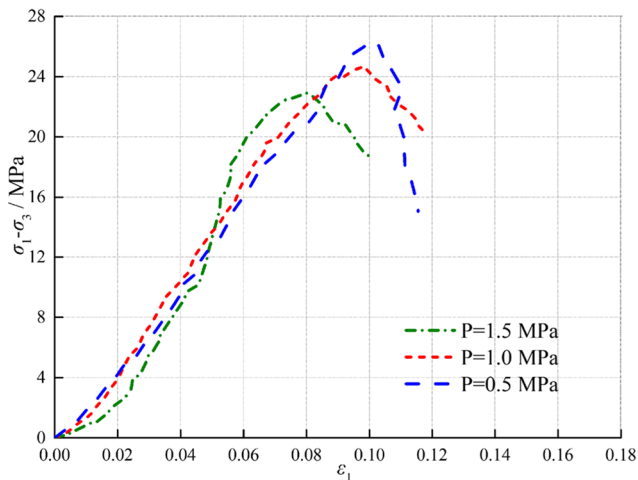
**b** Strain-permeability curve of  $\sigma_2$ -4 MPa



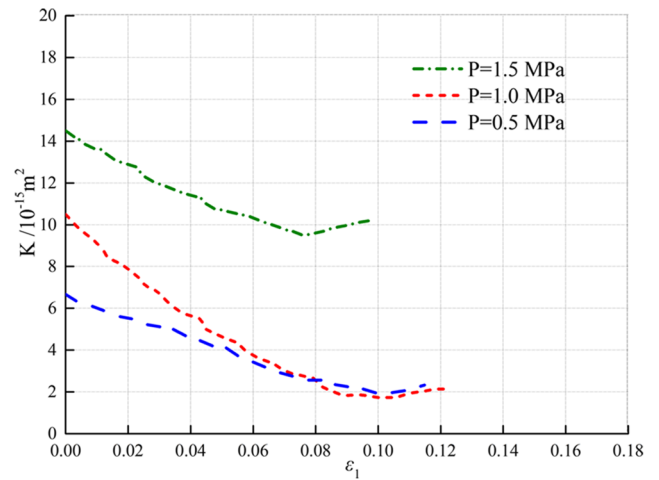
**c** Strain-stress curve of  $\sigma_2$ -6 MPa



**d** Strain-permeability curve of  $\sigma_2$ -6 MPa



**e** Strain-stress curve of  $\sigma_2$ -8 MPa



**f** Strain-permeability curve of  $\sigma_2$ -8 MPa

**Fig. 6** Axial strain-strain and strain-permeability curve of coal under different gas pressure loading. **a** Strain-stress curve of  $\sigma_2$ -4 MPa. **b** Strain-permeability curve of  $\sigma_2$ -4 MPa. **c** Strain-stress curve of  $\sigma_2$ -6

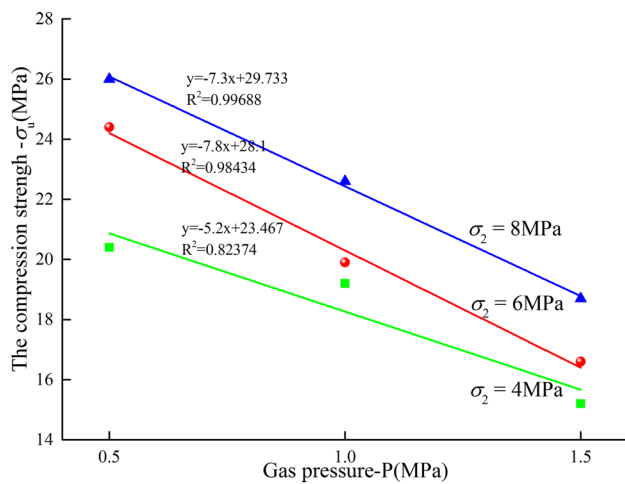
MPa. **d** Strain-permeability curve of  $\sigma_2$ -6 MPa. **e** Strain-stress curve of  $\sigma_2$ -8 MPa. **f** Strain-permeability curve of  $\sigma_2$ -8 MPa

2. With the increase of gas pressure, the gas pressure difference between the two ends of the coal sample is larger, the driving force to push gas through the coal sample also increases, the gas flow rate per unit time increases, and the gas permeation rate of the coal sample gradually increases. However, when the gas pressure increases to a certain extent and causes the coal body to produce obvious macroscopic deformation and damage, the mechanical effect of the gas pressure on the protruding coal body is close to the limit. Thus, further increasing in gas pressure has little effect on the internal cracks and pores. When the gas pressure distribution inside the coal sample is relatively uniform, the rate of increase of the gas permeation velocity at both ends of the coal sample will also approach a constant value.

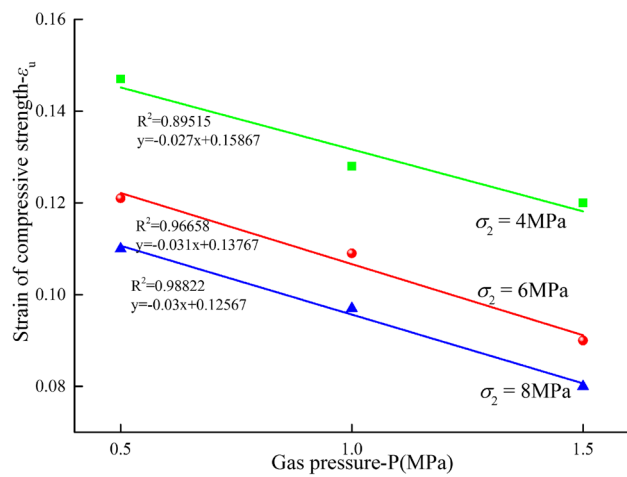
To sum up, at the same intermediate principal stress, the greater the gas pressure, the smaller the compressive

strength of the coal. But, relative to that at  $P$  equaling to 1.5 MPa, the compressive strength at  $P$  equaling to 0.5 MPa and 1.0 MPa only slightly decreased. The higher the gas pressure is, the greater the initial permeability. But,  $K_{min}$  at  $P$  equaling 0.5 MPa is similar to that at  $P$  equaling 1.0 MPa, indicating that at that condition,  $K_{min}$  is not increased with the increase of gas pressure. The reasons are as follows:

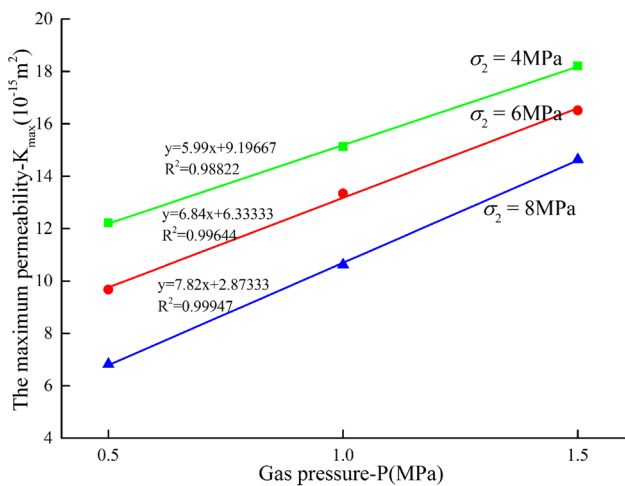
1. The effect of gas on the mechanical behavior of coal is mainly manifested as the pore pressure of the free gas in the specimen and the adsorption and expansion stress of the adsorbed gas, which have adverse effects on the mechanics characteristics of coal rock. But these effects are not obvious when gas pressure is lower than a certain value. Higher gas pressure promotes the development of micro-fractures in coal,



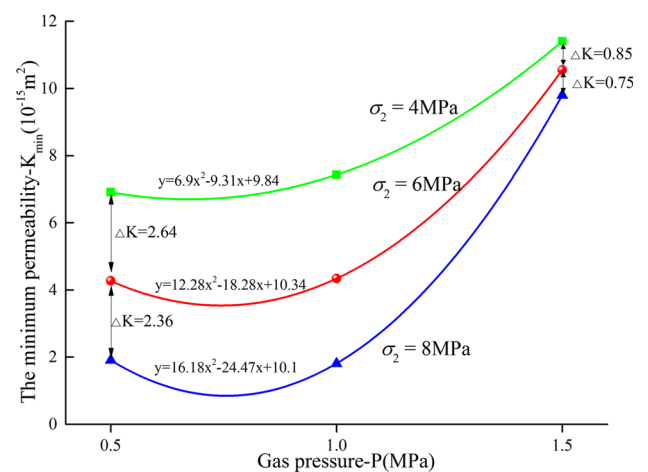
**a** the compression strength of coal



**b** the strain of coal



**c** the maximum permeability of coal



**d** minimum permeability of coal

**Fig. 7** Influence of gas pressure on coal mechanics and permeability characteristics. **a** The compression strength of coal. **b** The strain of coal. **c** The maximum permeability of coal. **d** The minimum permeability of coal

which weakens the strength of coal and makes it brittle and unstable.

- In addition, the same large gas pressure causes the pulverized coal particles to fall off and block the seepage channel to reduce the permeability of coal samples. The results show that the existence of gas pressure will not only reduce the strength of coal, but also reduce the deformation ability of coal. Therefore, when there is high gas pressure in underground coal mining, special attention should be paid to the effective release and extraction of gas pressure, so as to effectively avoid and prevent the occurrence of disaster caused by gas pressure.

From Figs. 4, 5, 6, and 7, it can be seen that each stress-strain curve rises to the maximum compressive strength and then decreases, while the permeability curve tends to be flat or slightly increased, but the change trend of Figs. 6 and 4 is obviously different: (1) in Fig. 4, when the gas pressure is the same and the stress environment is different, the slope of the stress-strain curve in three kinds of stress environment is obvious, but the slope of the permeability change curve is similar; (2) in Fig. 6, when the stress environment is the same and the osmotic gas pressure is different, the slope of the stress-strain curve of the three kinds of gas pressure grades is approximately the same; however, when the stress environment and the gas pressure are high, the large gas pressure will cause the coal body to instantaneously break sharply, resulting in an instantaneous increase in the slope of the stress-strain curve.

As can be seen from Figs. 5 and 7, the compressive strength, strain range, and maximum permeability of the coal body are more relaxed and have better regularity under the condition of three kinds of intermediate principal stress and gas pressure. However, the minimum permeability is in different stress environment and under different gas pressure, which shows a large variation range. Analysis of the reasons, when the intermediate principal stress and gas pressure are large, the coal body in the final stage of destruction, the extent of the damage shown is close. That is, after the destruction of coal body, the internal fracture development degree is similar. From Figs. 5d and 7d, in the same stress environment, when the gas pressure is lower than 1 MPa, the minimum permeability basically does not change much, and when it exceeds 1 MPa, the change is large. Under the same gas pressure condition, when the intermediate principal stress is low, the minimum permeability difference is larger. When the intermediate principal stress increases, the numerical difference becomes smaller and smaller. It shows that the higher intermediate principal stress is similar to the degree of coal body damage. The internal crack of the coal body in the residual strength stage develops to the limit; the expansion of the seepage channel is the same, and the minimum permeability barely changes.

## Conclusions

In this study, we use a self-developed “true triaxial gas-solid coupled coal seepage test system” to explore the seepage characteristic of briquette during the whole process of continuously loading constant minimum principal stress of 4 MPa and different intermediate principal stresses of 4 MPa, 6 MPa, and 8 MPa at gas pressure of 0.5 MPa, 1.0 MPa, and 1.5 MPa, respectively. The conclusions are listed below:

- In the conventional triaxial and true triaxial compression seepage tests, the stress-strain-permeability changes of the coal body are changed in stages, which are divided into the initial compaction stage, elastic deformation stage, plastic deformation stage, and destruction instability stage. The stress-strain curves in the whole stress-strain process of coal show a trend of decrease after increase, while the permeability-strain curves show a trend of increase after decrease.
- There is a “stress-sensitive zone” in the influence of the intermediate principal stress on the minimum permeability of the coal. When the gas pressure in the coal is the same, the  $\sigma_u$ ,  $\varepsilon$ ,  $K_{max}$ , and  $K_{min}$  of the coal body change linearly with the increase of the intermediate principal stress. However, when the intermediate principal stress is less than 6 MPa, the difference in the minimum permeability exhibited by the coal in different stress environments is small.
- The gas pressure promotes the “fluctuation” strain of the coal body, resulting in an instantaneous increase in the strain rate. The compressive strength of the coal body decreases as the gas pressure increases, and the maximum permeability is increased. However, when the gas pressure exceeds 1 MPa, the minimum permeability of the coal body is greatly increased and rises in a parabolic form.

**Funding information** This study was financially supported by the National Natural Science Foundation of China (project no. 51604168, 51474106), the Open Fund of Hebei State Key Laboratory of Mine Disaster Prevention (project no. KJZH2017K10), the Program for the Outstanding Young Scientists of Shandong University of Science and Technology (project no. 2015JQJH105), the Taishan Scholar Talent Team Support Plan for Advantaged and Unique Discipline Areas, and the Source Innovation Program (Applied Research Special—Youth Special) of Qingdao (project no. 17-1-1-38-jch).

## References

- Cao S-G, Guo P, Li Y, Bai Y-J, Liu Y-B, Xu J (2010) Effect of gas pressure on gas seepage of outburst coal. *J China Coal Soc* 35
- Chen Z, Liu J, Pan Z, Connell LD, Elsworth D (2012) Influence of the effective stress coefficient and sorption-induced strain on the

- evolution of coal permeability: model development and analysis. *Int J Greenh Gas Control* 8:101–110. <https://doi.org/10.1016/j.ijggc.2012.01.015>
- Chen Y, Zhang Y, Li X (2019) Experimental study on influence of bedding angle on gas permeability in coal. *J Pet Sci Eng* 179:173–179. <https://doi.org/10.1016/j.petrol.2019.04.010>
- Cheng W, Liu Z, Yang H, Wang W (2018) Non-linear seepage characteristics and influential factors of water injection in gassy seams. *Exp Thermal Fluid Sci* 91:41–53. <https://doi.org/10.1016/j.expthermflusci.2017.10.002>
- Ding Y, Yue ZQ (2018) An experimental investigation of the roles of water content and gas decompression rate for outburst in coal briquettes. *Fuel* 234:1221–1228. <https://doi.org/10.1016/j.fuel.2018.07.143>
- Dutka B (2019) CO<sub>2</sub> and CH<sub>4</sub> sorption properties of granular coal briquettes under in situ states. *Fuel* 247:228–236. <https://doi.org/10.1016/j.fuel.2019.03.037>
- Haimson B, Chang C (2000) A new true triaxial cell for testing mechanical properties of rock, and its use to determine rock strength and deformability of Westerly granite. *Int J Rock Mech Min Sci* 37:285–296. [https://doi.org/10.1016/S1365-1609\(99\)00106-9](https://doi.org/10.1016/S1365-1609(99)00106-9)
- He S, Jin L, Ou S, Ming X (2018) Soft coal solid—gas coupling similar material for coal and gas outburst simulation tests. *J Geophys Eng* 15:2033–2046. <https://doi.org/10.1088/1742-2140/aac098>
- Hu QT, Zhou SN, Zhou XQ (2013) Mechanical mechanism of coal and gas outburst process. Science Press, Beijing
- Jasinge D, Ranjith PG, Choi SK (2011) Effects of effective stress changes on permeability of latrobe valley brown coal. *Fuel* 90:1292–1300. <https://doi.org/10.1016/j.fuel.2010.10.053>
- Li W-X, Wang G, Du W-Z, Wang P-F, Chen J-H, Sun W-B (2016a) Development and application of a true triaxial gas-solid coupling testing system for coal seepage. *Yantu Rock Soil Mech* 37. <https://doi.org/10.16285/j.rsm.2016.07.036>
- Li M, Yin G, Xu J, Cao J, Song Z (2016b) Permeability evolution of shale under anisotropic true triaxial stress conditions. *Int J Coal Geol* 165:142–148. <https://doi.org/10.1016/j.coal.2016.08.017>
- Li XC, Zhang L, Li ZB, Jiang Y, Nie BS, Zhao YL, Yang C (2018) Creep law and model of coal under triaxial loading at different gas pressures. *J China Coal Soc* 43:473–482
- Liu W, Li Y, Wang B (2010) Gas permeability of fractured sandstone/coal samples under variable confining pressure. *Transp Porous Media* 83:333–347. <https://doi.org/10.1007/s11242-009-9444-8>
- Liu Y, Li M, Yin G, Zhang D, Deng B (2018) Permeability evolution of anthracite coal considering true triaxial stress conditions and structural anisotropy. *J Nat Gas Sci Eng* 52:492–506. <https://doi.org/10.1016/j.jngse.2018.02.014>
- Lombos L, Roberts DW, King M, (2013) Design and development of integrated true triaxial rock testing, in: *True triaxial testing of rocks*. pp. 35–49.
- Mavor M, Gunter W (2006) Secondary porosity and permeability of coal vs. gas composition and pressure. *SPE Reserv Eval Eng* 9:26–29. <https://doi.org/10.2118/90255-PA>
- Meng J, Nie B, Zhao B, Ma Y (2015) Study on law of raw coal seepage during loading process at different gas pressures. *Int J Min Sci Technol* 25:31–35. <https://doi.org/10.1016/j.ijmst.2014.12.005>
- Mogi K (1967) Effect of the intermediate principal stress on rock failure. *J Geophys Res* 72:5117–5131. <https://doi.org/10.1016/j.coal.2016.08.017>
- Mogi K (1971) Fracture and flow of rocks under high triaxial compression. *J Geophys Res* 76:1255–1269
- Pan PZ, Feng XT, Hudson JA (2012) The influence of the intermediate principal stress on rock failure behaviour: a numerical study. *Eng Geol* 124:109–118. <https://doi.org/10.1016/j.enggeo.2011.10.008>
- Qin H, Huang G, Jiang C, Li W (2013) Experimental research on acoustic emission characteristics of coal and rock under different gas pressures. *Chin J Rock Mech Eng* 32
- Shi L, Zeng Z, Bai B, Li X (2018) Effect of the intermediate principal stress on the evolution of mudstone permeability under true triaxial compression. *Greenh Gases* 50:37–50. <https://doi.org/10.1002/ghg.1732>
- Wang FZ, Qian DL (2018) Elasto-analysis for a deep tunnel considering intermediate stress and. *J China Coal Soc* 43:3329–3337
- Wang G, Cheng W-M, Guo H, Long Q-M (2012) Study on permeability characteristics of coal body with gas pressure variation. *J Min Saf Eng* 29
- Wang K, Du F, Wang G (2017a) Investigation of gas pressure and temperature effects on the permeability and steady-state time of Chinese anthracite coal: an experimental study. *Int J Rock Mech Min Sci* 40:179–188. <https://doi.org/10.1016/j.jngse.2017.02.014>
- Wang G, Li W, Wang P, Yang X, Zhang S (2017b) Deformation and gas flow characteristics of coal-like materials under triaxial stress conditions. *Int J Rock Mech Min Sci* 91:72–80. <https://doi.org/10.1016/j.ijrmms.2016.11.015>
- Wang G, Wang P, Guo Y, Li W (2018) A novel true triaxial apparatus for testing shear seepage in gas-solid coupling coal. *Geofluids* 2018:1–9
- Wang G, Guo Y, Du C, Sun L, Liu Z, Wang Y, Cao J (2019) Experimental study on damage and gas migration characteristics of gas-bearing coal with different pore structures under sorption-sudden unloading of methane 2019
- Wenshuai LI, Lianguo W, Yinlong LU, Zhaolin LI (2019) Experimental investigation on the strength, deformation and failure characteristics of sandstone under true triaxial compression. *J Min Saf Eng* 36(36):191–197. <https://doi.org/10.13545/j.cnki.jmse.2019.01.025>
- Xu J, Peng S, Yin G, Tao Y, Yang H, Wang W (2010) Development and application of triaxial servo-controlled seepage equipment for thermo-fluid-solid coupling of coal containing methane. *Yanshilixue Yu Gongcheng Xuebao/Chinese J. Rock Mech. Eng.* 29.
- Yin G, Li G, Zhao H, Li X, Jing X, Jiang C (2010) Experimental research on gas flow properties of coal specimens in complete stress-strain process. *Chin J Rock Mech Eng* 29
- Yin G, Jiang C, Xu J, Guo L, Peng S, Li W (2012) An experimental study on the effects of water content on coalbed gas permeability in ground stress fields. *Transp Porous Media* 94:87–99. <https://doi.org/10.1007/s11242-012-9990-3>
- Yin G, Li M, Wang JG, Xu J, Li W (2015) Mechanical behavior and permeability evolution of gas infiltrated coals during protective layer mining. *Int J Rock Mech Min Sci* 80:292–301. <https://doi.org/10.1016/j.ijrmms.2015.08.022>
- Yin G, Jiang C, Xu JGWJ, Zhang D (2016) A new experimental apparatus for coal and gas outburst simulation. *Rock Mech Rock Eng* 49:2005–2013. <https://doi.org/10.1007/s00603-015-0818-7>
- Yin G, Deng B, Li M, Zhang D, Wang W, Li W, Shang D (2017) Impact of injection pressure on CO<sub>2</sub>-enhanced coalbed methane recovery considering mass transfer between coal fracture and matrix. *Fuel* 196:288–297. <https://doi.org/10.1016/j.fuel.2017.02.011>
- Zhang ZP, Gao MZ, Zhang ZT, Zhang R, Li G (2015) Research on permeability characteristics of raw coal in complete stress-strain process under different gas pressure. *J China Coal Soc* 40:836–842